



HAL
open science

CaV3.2 T-type Calcium Channels Are Involved in Calcium-dependent Secretion of Neuroendocrine Prostate Cancer Cells

Florian Gackière, Gabriel Bidaux, Philippe Delcourt, Fabien van Coppenolle, Maria Katsogiannou, Etienne Dewailly, Alexis Bavencoffe, Myriam Tran van Chuoï-Mariot, Brigitte Mauroy, Natalia Prevarskaya, et al.

► **To cite this version:**

Florian Gackière, Gabriel Bidaux, Philippe Delcourt, Fabien van Coppenolle, Maria Katsogiannou, et al.. CaV3.2 T-type Calcium Channels Are Involved in Calcium-dependent Secretion of Neuroendocrine Prostate Cancer Cells. *Journal of Biological Chemistry*, 2008, 283 (15), pp.10162-10173. 10.1074/jbc.M707159200 . hal-03060261

HAL Id: hal-03060261

<https://hal.science/hal-03060261>

Submitted on 13 Dec 2020

HAL is a multi-disciplinary open access archive for the deposit and dissemination of scientific research documents, whether they are published or not. The documents may come from teaching and research institutions in France or abroad, or from public or private research centers.

L'archive ouverte pluridisciplinaire **HAL**, est destinée au dépôt et à la diffusion de documents scientifiques de niveau recherche, publiés ou non, émanant des établissements d'enseignement et de recherche français ou étrangers, des laboratoires publics ou privés.



Distributed under a Creative Commons Attribution 4.0 International License

CaV3.2 T-type Calcium Channels Are Involved in Calcium-dependent Secretion of Neuroendocrine Prostate Cancer Cells*

Received for publication, August 27, 2007, and in revised form, January 10, 2008. Published, JBC Papers in Press, January 29, 2008, DOI 10.1074/jbc.M707159200

Florian Gackière, Gabriel Bidaux, Philippe Delcourt, Fabien Van Coppenolle, Maria Katsogiannou, Etienne Dewailly, Alexis Bavencoffe, Myriam Tran Van Chuoi-Mariot, Brigitte Mauroy, Natalia Prevarskaya, and Pascal Mariot¹

From the INSERM, U800, Laboratoire de Physiologie Cellulaire, Equipe Labellisée par la Ligue contre le Cancer and Université des Sciences et Technologies de Lille, Villeneuve d'Ascq, 59650, France

Because prostate cancer is, in its early stages, an androgen-dependent pathology, treatments aiming at decreasing testosterone plasma concentration have been developed for many years now. However, a significant proportion of patients suffer a relapse after a few years of hormone therapy. The androgen-independent stage of prostate cancer has been shown to be associated with the development of neuroendocrine differentiation. We previously demonstrated that neuroendocrine prostate cancer cells derived from LNCaP cells overexpress CaV3.2 T-type voltage-dependent calcium channels. We demonstrate here using prostatic acid phosphatase as a marker of prostate secretion and FM1-43 fluorescence imaging of membrane trafficking that neuroendocrine differentiation is associated with an increase in calcium-dependent secretion which critically relies on CaV3.2 T-type calcium channel activity. In addition, we show that these channels are expressed by neuroendocrine cells in prostate cancer tissues obtained from patients after surgery. We propose that CaV3.2 T-type calcium channel up-regulation may account for the alteration of secretion during prostate cancer development and that these channels, by promoting the secretion of potential mitogenic factors, could participate in the progression of the disease toward an androgen-independent stage.

Prostate cancer is, in its early stages, an androgen-dependent pathology, meaning that its progression relies on the presence of active steroid male hormones. Treatments developed for many years have been based on this characteristic feature of prostate cancer and, thus, aimed at decreasing the plasma concentration of testosterone or dihydrotestosterone, the prostate active androgen. Although these treatments are particularly valuable in the early development of the disease, leading to the regression of cancers, about a third of the patients suffer a relapse after a few years of hormone therapy. At this stage of

hormone refractory disease, deprivation of androgens has no further incidence on the growth of the prostate cancer, and no curative therapy is currently effective (for review, see Ref. 1).

The androgen-independent stage of prostate cancer has been shown to be associated with, among others, the development of neuroendocrine differentiation (2). These neuroendocrine features include the appearance of neuroendocrine cell foci surrounded by proliferating epithelial cells (3). Because neuroendocrine prostate cells in normal, hyperplastic, or cancerous tissue secrete many neuropeptides with mitogenic activities like parathyroid hormone-related peptide, calcitonin, or gastrin-related peptides, it has been proposed that paracrine secretion of neurosecretory products released by neuroendocrine cells could be responsible for the progression of cancer toward an androgen-independent stage (for review, see Ref. 4). Indeed, it has been shown for instance that the expression of neuroendocrine markers like chromogranin A is correlated with tumor dedifferentiation (5) and that the presence of neuroendocrine cells in prostate cancer is correlated to a negative prognosis (6). Furthermore, it has been shown that neuroendocrine cells lack the androgen receptor (4, 7), thereby constituting an androgen-independent compartment of prostate tumors.

A neuroendocrine differentiation model has been developed using LNCaP cells whose differentiation can be induced by various means, e.g. activation of the protein kinase A pathway, interleukin-6 receptor activation, or steroid depletion (8–10). Neuroendocrine differentiation of LNCaP cells is associated with modifications of the morphological phenotype such as neuritic extensions, secretory granules, and the over- (or neo-) expression of molecular markers (neuron-specific enolase, chromogranin, neurotensin, parathyroid hormone-related peptide). In a previous study (11), we have demonstrated that neuroendocrine prostate LNCaP cells (LNCaP-NE) overexpress a voltage-dependent calcium current of the T-type family. The channel subunit involved in this calcium current was shown to be the CaV3.2 (α_{1H}) pore subunit. The role of this calcium channel in allegedly non-excitable cells remains elusive. We supposed from morphological evidence that the T-type calcium channel was involved in the extension of neurites during the neuroendocrine differentiation process. In other cell models, the T-type calcium channel function has been attributed to pacemaker activity, gene expression, or development. In recent studies T-type calcium currents have been shown to be responsible for exocytosis in acrosomal reaction (12) or synaptic transmis-

* This work was supported by INSERM, the Ligue Nationale contre le Cancer (Comité du Nord), and the Université of Sciences et Technologies de Lille. The costs of publication of this article were defrayed in part by the payment of page charges. This article must therefore be hereby marked "advertisement" in accordance with 18 U.S.C. Section 1734 solely to indicate this fact.

¹ To whom correspondence should be addressed: Laboratoire de Physiologie Cellulaire, INSERM U800, Bâtiment SN3, Université des Sciences et Technologies de Lille, 59655 Villeneuve d'Ascq Cédex, France. Tel.: 33-03-20-43-40-77; Fax: 33-03-20-43-40-66; E-mail: Pascal.Mariot@univ-lille1.fr.

sion in neurons or chromaffin cells (13–15). Because neuroendocrine LNCaP cells have been shown to secrete more neuropeptides than non-differentiated LNCaP cells, we investigated both whether a calcium-dependent-regulated pathway was present in these cells and the putative role of T-type calcium channels in the secretion of LNCaP cells. We show in this article that LNCaP cells display a calcium-dependent pathway of regulated secretion and that neuroendocrine differentiation is associated with an increase in prostatic acid phosphatase (PAP)² secretion. We also show that T-type calcium channels could promote secretion upon membrane depolarization and that PAP secretion by LNCaP cells is dependent on T-type (α_{1H}) calcium channel activity. In addition, we show that prostate cancer cells obtained after surgical removal of prostate biopsies express functional α_{1H} T-type calcium channels. Furthermore, we demonstrate for the first time that these channels colocalize with serotonin and chromogranin A neuroendocrine markers and cytokeratin 18, which shows the epithelial neuroendocrine nature of CaV3.2-expressing cells and are more abundant in human prostate cancer tissue samples than in hyperplasia.

EXPERIMENTAL PROCEDURES

Cell Culture and Treatments—LNCaP cells were cultured as previously described (11). To induce neuroendocrine differentiation, LNCaP cells were cultured with 1 mM dibutyryl cyclic AMP and 100 μ M isobutylmethylxanthine for 3–6 days. Stable cell lines expressing α_{1H} protein (LNCaP- α_{1H}) or α_{1H} -GFP fusion protein (LNCaP- α_{1H} -GFP) or control LNCaP cell lines transfected with an empty pcDNA3 vector (LNCaP-Neo) were produced as previously reported (16). Epithelial cells from benign prostate hyperplasia (BHP cells) and from prostate carcinomas (hPCE cells) in primary culture were obtained and maintained in culture as previously described (17, 18). Human prostate tissue specimens were obtained from resection surgeries performed on patients who gave informed consent and on clinical indications in the Urology Department at l'Hôpital St. Philibert. All experiments on human tissues were approved by the Comité Consultatif de Protection des Personnes dans la Recherche Biomedicale de Lille, Lille, France.

Fluorescence Imaging—Fluorescence imaging was carried out in Hank's balanced salt solution (HBSS) containing 142 mM NaCl, 5.6 mM KCl, 1 mM MgCl₂, 2 mM CaCl₂, 0.34 mM Na₂HPO₄, 0.44 mM KH₂PO₄, 10 mM HEPES, and 5.6 mM glucose. The osmolarity and pH of external solutions were adjusted to 310 mosmol.liter⁻¹ and 7.4, respectively.

Cytosolic calcium concentration was measured using Fura2-loaded cells (2 μ M) as described elsewhere (11). The intracellular calcium concentration was derived from the ratio of the fluorescence intensities for each of the excitation wavelengths (F340/F380) and from the Grynkiewicz *et al.* (19) equation. The

cells were continuously perfused with the HBSS solution, and chemicals were added via a perfusion system.

FM1-43 fluorescence was used as indicative of membrane traffic (20, 21). When cells are bathed in FM1-43 solution (5 μ M), the dye (non-fluorescent in aqueous solution) is incorporated into the plasma membrane until equilibrium has been reached. The dye then becomes fluorescent in the lipid membrane environment. Fluorescence was excited at 480 nm and measured at 510 nm. TMA-DPH (1 μ M) was also used as an indicator of membrane traffic as previously reported (22). Fluorescence protocols were essentially the same as with FM1-43.

Because Fura2 and FM1-43 spectra do not cross over, combined Fura2 and FM1-43 measurements were performed as done by others (23). Fluorescence was alternately excited at 340, 380, and 480 nm and measured at 510 nm. All recordings were carried out at 35 °C.

Electrophysiological Recordings—Patch clamp recordings were performed in the whole-cell configuration as previously described (24) using a RK-300 patch clamp amplifier (Biologic, Grenoble, France).

Bath medium used for voltage clamp experiments contained 142 mM NaCl, 1 mM MgCl₂, 10 mM HEPES, 5.6 mM glucose, 10 mM tetraethyl ammonium chloride, and 2 mM CaCl₂. The osmolarity and pH of external buffers were adjusted to 310 mosmol.liter⁻¹ and 7.4, respectively. Recording pipettes were filled with a solution containing 140 mM *N*-methyl glucamine, 110 mM L-glutamic acid, 30 mM HCl, 5 mM HEPES, 1 mM MgCl₂, with 0.1 or 1 mM EGTA. Osmolarity and pH were adjusted to 290 mosmol.liter⁻¹ and 7.2, respectively.

In some experiments voltage clamp experiments were combined on the same cell to calcium or FM1-43 imaging. Patch clamp experiments were carried out at room temperature except combined experiments which were performed at 35 °C.

Confocal Microscopy—Confocal fluorescence analysis was performed using a Zeiss LSM 510 confocal microscope (Carl Zeiss, Le Pecq, France) connected to a Zeiss Axiovert 200M with a \times 63 oil-immersion objective lens (numerical aperture 1.4). For quantification analysis, the image acquisition characteristics (*i.e.* pinhole aperture, laser intensity, scan speed) were the same throughout the experiments to ensure the comparability of the results. AIM 3.2 confocal microscope software (Carl Zeiss) was used for data acquisition and analysis. Changes in FM1-43 fluorescence were monitored by excitation with a 477 nm line of a 20-milliwatt argon ion laser, and emission from the dye was collected through a 505-nm long-pass filter.

Confocal immunofluorescence experiments were performed with an \times 40 oil-immersion objective lens (numerical aperture 1.2) and illuminated separately with an argon ion laser and an helium/neon ion laser. 0.7- μ m confocal slides were scanned to determine the localization of the targeting proteins.

Immunofluorescence—1) LNCaP cells were fixed with 4% formaldehyde, 1 \times phosphate-buffered saline (PBS) for 15 min, washed 3 times, then permeabilized in PBS, 1.2% gelatin complemented with 0.01% Tween 20 and 100 mM glycine for 30 min at 37 °C. 2) Resection specimens from human prostate were frozen in liquid nitrogen-cooled isopentane and kept in "Tissue-Tek®" at -80 °C before 10- μ m sections were prepared at -20 °C with a cryostat and mounted on glass slides. The sec-

² The abbreviations used are: PAP, prostatic acid phosphatase; cPAP, intracellular PAP; sPAP, secreted PAP; HBSS, Hank's balanced salt solution; PBS, phosphate-buffered saline; TG, thapsigargin; PMA, phorbol 12-myristate 13-acetate; CK18, cytokeratin 18; GFP, green fluorescent protein; BHP, benign prostate hyperplasia; DIFMUP, 6,8-difluoro-4-methylumbelliferyl phosphate; siRNA, small interfering RNA; PSA, prostate-specific antigen; TMA-DPH, 1-(4-(trimethylamino)phenyl)-6 phenylhexa-1,3,5-triene.

T-type Calcium Channels and Prostate Cancer Secretion

tions were blocked with PBS, 1.2% gelatin complemented with 0.01% Tween 20 for 30 min at 37 °C.

Samples were then incubated with primary antibodies: (1:500) rabbit polyclonal anti-Cav3.2 antibody (Alomon Labs), (1:200) mouse monoclonal anti-Serotonin antibody (Dako), (1:50) mouse monoclonal anti-chromogranin A antibody (Dako), (1:1000) mouse monoclonal anti-cytokeratin 18 antibody (Neomarkers), in PBS-gelatin completed with 5% donkey serum and 0.5% Triton X-100 at 37 °C for 1.5 h. After thorough washes, the slides were treated with the corresponding anti-rabbit or anti-mouse IgG coupled with either Alexa fluor 546-labeled (Molecular Probes, dilution 1:4000) or Alexa fluor 488-labeled (dilution 1:2000) diluted in PBS-gelatin for 1 h at room temperature. After 2 washes in PBS and a last wash in PBS + 1:200 4',6-diamidino-2-phenylindole for 15 min, the slides were mounted with Mowiol®.

Prostatic Acid Phosphatase Secretion—For the PAP assay, we used two methods. The first is a Sigma colorimetric procedure (Sigma, unit·ml⁻¹) in which *p*-nitrophenol phosphate was used as the substrate to quantify the acid phosphatase activity at pH 4.8 by measuring the absorbance of released *p*-nitrophenol at 405 nm (25). Sigma units were transformed in IU·ml⁻¹ according to the Sigma protocol (1 sigma unit·ml⁻¹ equals 16.7 mIU·ml⁻¹. Sigma protocol sheet). The second method is a sensitive fluorimetric assay (Molecular Probes, mIU·ml⁻¹) based on the cleavage of 6,8-difluoro-4-methylumbelliferyl phosphate (DIFMUP) by phosphatases (26), generating DIFMU, whose fluorescence was excited at 360 nm and measured at 450 nm. In prostate cells the L(+)-tartrate-sensitive acid phosphatase activity has conventionally been used to represent PAP activity (25).

Viability Tests—Cell viability was assessed by a colorimetric method (CellTiter 96 Aqueous Non-Radioactive Cell Proliferation Assay, Promega).

siRNA Design and Cell Preparation—Small interfering RNAs against the human coding sequence of Cav3.2 calcium channels (GenBank™ accession number NM-021098.2) were designed, and two selective sequences, referred to as si- $\alpha_{1H}1$ and si- $\alpha_{1H}2$, were selected to knock down T-type α_{1H} calcium channel expression. siRNAs used in this study included a nonspecific siRNA (si-Ctl) control with at least four mismatches with any human genes. Sense sequences of siRNAs were 5'-UAGCGACU-AAACACAUCAA-3' (si-Ctl), 5'-ACGUGAGCGCAUGCUG-GUAAUdTdT-3' (si- $\alpha_{1H}1$, position 311–329 from ATG), and 5'-AGAUGGCCGUGGCGUCUAUdTdT-3' (si- $\alpha_{1H}2$, position 2166–2184 from ATG). siRNAs were purchased from Dharmacon (France).

LNCaP-CTL, LNCaP- α_{1H} , or LNCaP- α_{1H} GFP cells were transfected with either 5, 25, or 50 nM siRNA anti- $\alpha_{1H}1$, anti- $\alpha_{1H}2$, or siRNA-Ctl using HiPerFect Transfection Reagent (Qiagen). siRNAs were incubated in culture medium without serum for 5–10 min at room temperature to form the transfection complexes and were then added dropwise onto the cells. The medium was then changed as required, and gene silencing could be studied after an appropriate time depending on experimental set-up.

Analysis of the α_{1H} Subunit Gene Expression of a Voltage-dependent T-type Calcium Channel (Reverse Transcription-PCR)—Reverse transcription-PCR was carried out as previously described (16). The PCR primers used to amplify the 177-bp

α_{1H} amplicon were 5'-TCGAGGAGGACTTCCACAAG (forward) and 5'-TGCATCCAGGAATGGTGAG (reverse), and those used to amplify the 220-bp β -actin amplicon were 5'-CAGAGCAAGAGAGGCATCCT-3' (forward) and 5'-ACGT-ACATGGCTGGGGTGTGAA-3' (reverse).

Western Blot Assay—Western blot analysis of protein expression in LNCaP-NE or LNCaP- α_{1H} GFP cells (control or siRNA-transfected) were designed as described elsewhere (11). Primary antibodies used in this study were anti-GFP (1:1000, rabbit, Abcam), anti-PAP (1:100, rabbit, Interchim), anti- β -actin (1:400, mouse, Sigma), or anti-calnexin (1:1000, mouse, Chemicon International, Inc.).

Chemicals—All chemicals were purchased from Sigma except for Fura2-AM which was bought from Calbiochem.

Statistical Analysis—Results are expressed as the mean \pm S.E. Statistical analysis was performed using unpaired *t* tests (for comparing two groups) or analysis of variance tests followed by either Dunnett (for multiple control *versus* test comparisons) or Student-Newman-Keuls post-tests (for multiple comparisons). Differences were considered significant where $p < 0.05$ (*), $p < 0.01$ (**), and $p < 0.001$ (***)

RESULTS

Calcium-dependent secretion was first investigated on LNCaP cell populations, and the concentration of prostatic-specific PAP in the incubation medium was used as an index of exocytotic secretion because PAP was shown to be distributed in secretory granules (8). To assess whether PAP secretion could be stimulated by a calcium rise, we incubated the cells with various agents raising cytosolic calcium like thapsigargin (TG, an inhibitor of endoplasmic reticulum Ca²⁺ ATPases) or ionomycin (a calcium ionophore) and with different external calcium concentrations (0, 0.75, or 1.5 mM CaCl₂). As shown in Fig. 1A, the amount of PAP measured with a colorimetric assay increased in both cell lysates and culture media when stimulated by either TG or ionomycin. In addition, TG- or ionomycin-induced secretion was blocked by removing calcium from the culture medium (Fig. 1A) or was potentiated by increasing the calcium concentration from 0.75 to 1.5 mM (not shown). Using DIFMUP as a PAP substrate, we were able to detect PAP secretion within 30 min of incubation. As shown in Fig. 1B, a 30-min incubation period in a culture medium containing 0.75 mM CaCl₂ with TG and ionomycin almost doubled the amount of PAP secreted in the culture medium (control 3.1 \pm 0.7, ionomycin 5.6 \pm 0.6, TG 4.7 \pm 0.4, 10⁻³ IU·ml⁻¹). To clamp external calcium concentrations more efficiently (0–5 mM), we carried out some experiments in HBSS. Basal PAP secretion increased in the presence of 5 mM calcium (3.4 \pm 0.2 10⁻³ IU·ml⁻¹ in calcium-free conditions *versus* 6.2 \pm 0.3 10⁻³ IU·ml⁻¹ in 5 mM external calcium, Fig. 1C). Furthermore, ionomycin-stimulated PAP secretion required the presence of calcium in the external medium. In addition, when LNCaP cells were treated with protein synthesis inhibitors (cycloheximide (200 μ M) and anisomycin (300 μ M)), the amount of PAP released in the incubation medium after 1 h was not altered in either basal or stimulated conditions (2 μ M ionomycin). In contrast, PAP secreted in the culture medium after 24 h of incubation was abrogated by protein synthesis inhibition (Fig. 1D) in

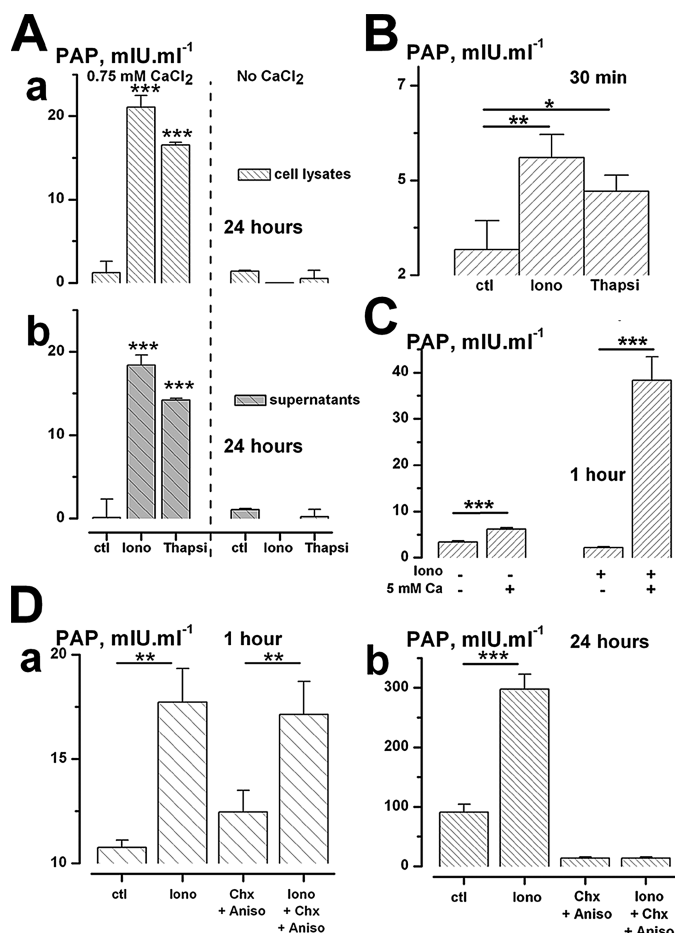


FIGURE 1. Calcium-dependent secretion of PAP by LNCaP cells. A, PAP was measured with a colorimetric assay (using *p*-nitrophenol phosphate as a substrate) in the cell lysates after permeabilization with TritonX100 (0.1%) (a) and in supernatants (b). Cells were cultured in standard RPMI medium (left panels) or in calcium-free RPMI (right panels) and were submitted to ionomycin (*lono*, 2 μ M) or thapsigargin (*Thapsi*, 10 nM) treatments for 24 h. *ctl*, control. B and C, using a fluorogenic substrate of PAP (DIFMUP), secretion of PAP induced by ionomycin or thapsigargin could be measured after only 30 min in RPMI (B) or 60 min in HBSS (C) incubation in the different stimuli. D, PAP was measured using DIFMUP. LNCaP cells were treated for 2 h with cycloheximide (*Chx*, 200 μ M) and anisomycin (*Aniso*, 300 μ M) to block protein synthesis. LNCaP cells were then further incubated in ionomycin (2 μ M) for 1 (a) or 24 h (b) in the presence of protein synthesis inhibitors. Protein synthesis inhibition did not impair calcium-dependent PAP secretion after a 1-h incubation period but strongly inhibited both basal and calcium-activated PAP secretion in long-term experiments.

both basal and stimulated conditions. Ionomycin and thapsigargin at the concentrations used in this study (1–2 μ M for ionomycin and 10–20 nM for thapsigargin) did not induce any significant cell death nor any increase in cell proliferation (not shown) within 48 h, which could have been responsible for any apparent variations in PAP concentrations.

To further investigate the calcium-dependent secretion of LNCaP cells, we carried out fluorescence imaging of FM1-43 and TMA-DPH, fluorescent lipophilic dyes used for tracking membrane traffic (for review, see Refs. 20 and 21). When FM1-43 was admitted into the perfusion chamber, cell fluorescence progressively reached a stable level. At this stage, as observed in both conventional imaging and confocal microscopy (Fig. 2A), FM1-43 fluorescence was preferentially localized at the cell periphery, indicating plasma membrane location. When admitted into the

bath, ionomycin (2 μ M) rapidly increased FM1-43 or TMA-DPH fluorescence (see Fig. 2). On average, ionomycin increased FM1-43 fluorescence by $106 \pm 7\%$ ($n = 150$) and $38 \pm 2\%$ ($n = 97$) in the presence and absence of extracellular calcium, respectively. Similarly, thapsigargin (20 nM) induced a rise in FM1-43 fluorescence of $31 \pm 2\%$ ($n = 106$) and $15 \pm 6\%$ ($n = 32$) in the presence and absence of extracellular calcium, respectively. Combined Fura2 and FM1-43 fluorescence measurements (Fig. 2B) show that ionomycin and thapsigargin induced cytosolic calcium peaks that were rapidly followed by increases in FM1-43 fluorescence. In some cases, ionomycin-induced calcium peaks were biphasic, and the increase in FM1-43 fluorescence correlated with either of the calcium transients. In any cases, as emphasized on Fig. 2B, the sharpest rise in FM1-43 fluorescence occurred during the rising phase of the calcium peaks.

Because FM1-43 is able to be progressively incorporated in intracellular membrane organelles such as secretory granules through endocytosis (20, 21), we incubated LNCaP cells overnight in 5 μ M FM1-43 diluted in culture medium. Then, cells were washed with FM1-43 free HBSS to remove FM1-43 from the plasma membrane. The dye was incorporated into intracellular membrane compartments as shown by confocal microscopy by a punctuated fluorescence inside the cell (Fig. 2E). When submitted to 1 μ M ionomycin, the FM1-43 fluorescence inside the cell decreased after a 1-min time lag (% of decrease ($\Delta F/F_0$) = 8.7 ± 2.2 , $n = 68$). This probably reflects the release by exocytosis of FM1-43 previously incorporated by membrane retrieval in intracellular organelle membranes such as secretory granules. This demonstrates that FM1-43 incorporates at least partially into immediately releasable secretory pools and, thus, confirms that FM1-43 is a good LNCaP cell membrane traffic marker.

Neuroendocrine differentiation of LNCaP prostate cancer cells, induced by treatments increasing cytosolic cAMP, was shown to be associated with an increase in neuropeptide secretion (27). In the present study PAP secreted in the incubation medium for 1 h increased in both basal (by $36 \pm 1.2\%$) and ionomycin-stimulated (by $48 \pm 3.5\%$) conditions in neuroendocrine LNCaP cells (LNCaP-NE) as compared with undifferentiated LNCaP cells (LNCaP-CTL), confirming an increase in secretory potency after neuroendocrine differentiation. Furthermore, we show by immunofluorescence confocal detection (Fig. 3) that LNCaP-NE cells express chromogranin A, a marker of regulated secretion, and serotonin (5-HT), a neurotransmitter.

We then carried out experiments to assess whether α_{1H} (CaV3.2) T-type calcium channels could be involved in PAP secretion. Indeed, as previously published (11, 16) and as displayed on Fig. 3, LNCaP-NE cells have an increased expression of T-type calcium currents. We show here using a CaV3.2 antibody that LNCaP-NE cells indeed overexpress CaV3.2 calcium channels (Fig. 3). We conducted experiments using T-type calcium channel inhibitors and small interfering RNAs raised against α_{1H} channels (two different sets of siRNA: si- α_{1H1} and si- α_{1H2}). CaV3.2 T-type calcium channels overexpressed in LNCaP cells could be inhibited by flunarizine (89.5% inhibition at 10 μ M, $n = 10$), nickel chloride (45% inhibition at 20 μ M, $n = 10$), and kurtoxin (92.3% inhibition at 500 nM, $n = 10$) (data not shown). To validate the siRNAs used in this study, we have shown using patch clamp experiments in LNCaP stably trans-

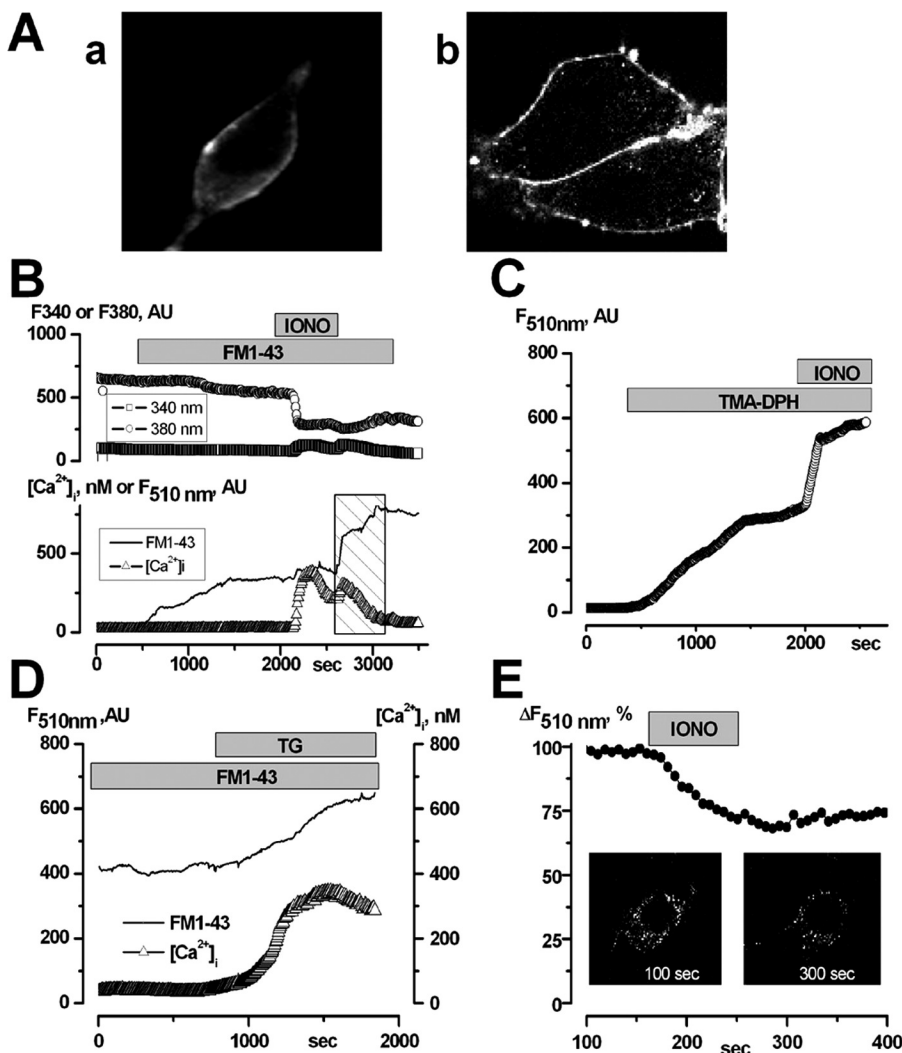


FIGURE 2. Fluorescence imaging of FM1-43. *A*, conventional video (*a*) and confocal (*b*) imaging of LNCaP cells in the presence of 5 μM FM1-43 in the bath. As shown by these pictures, most of the fluorescence is located in the plasma membrane. *B*, time lapse video-imaging of FM1-43 and Fura2 fluorescence were measured on a single LNCaP cell. As shown, there was no fluorescence cross-variations of either dye. Ionomycin (*iono*) induced a calcium rise followed by an increase in FM1-43 fluorescence after a short delay. *C*, a similar experiment conducted with another membrane dye, TMA-DPH (1 μM). *D*, TG induced a similar increase in FM1-43 fluorescence in an LNCaP cell. *E*, dynamic confocal measurement of FM1-43 fluorescence in an LNCaP cell preloaded with FM1-43 (5 μM) for 12 h. FM1-43 was removed from the perfusion solution before the experiment. FM1-43 fluorescence appeared as a punctuated pattern inside the cell showing that FM1-43 had been trapped inside intracellular compartments. FM1-43 fluorescence decreased upon application of 2 μM ionomycin.

ected with α_{1H} -GFP (LNCaP- α_{1H} GFP) that the expression of T-type calcium currents was inhibited with siRNA concentrations as low as 5 nM (Fig. 4A). Indeed, inhibition was already maximal at 5 nM with both si- α_{1H1} and si- α_{1H2} 48 h after siRNA treatment. The inhibition began to reverse 4 and 7 days after the onset of siRNAs treatment for si- α_{1H1} and si- α_{1H2} , respectively. In addition, a decrease in protein expression after si- α_{1H} treatments was observed on Western blots using an anti-GFP antibody in LNCaP- α_{1H} -GFP cells (Fig. 4B) and in immunofluorescence confocal detection experiments using a anti-CaV3.2 antibody in LNCaP cells stably transfected with α_{1H} (LNCaP- α_{1H} , Fig. 4C). In LNCaP-NE cells (Fig. 4A), T-type calcium currents were about 20 times smaller than in LNCaP- α_{1H} cells and were inhibited by both siRNAs (si- α_{1H1} and si- α_{1H2} , 5 nM) 3–4 days after siRNA treatment. At concentrations up to 100 nM, control siRNA (si-Ctl) was ineffective in decreasing the magni-

tude of T-type calcium currents in both LNCaP- α_{1H} and LNCaP-NE cells.

We, therefore, tested the action of these siRNAs on basal PAP secretion by LNCaP-NE cells. We used siRNAs at 5 nM for secretion assays because at this concentration none of the siRNAs used in our study had any effect on cell viability (see Fig. 5A). In the experiment shown in Fig. 5A, basal secretion of PAP was inhibited by about 25 and 50% by si- α_{1H1} and si- α_{1H2} , respectively. On average, si- α_{1H1} and si- α_{1H2} , but not si-Ctl, inhibited basal PAP secretion by 28 ± 3.5 and $27.4 \pm 6.4\%$ ($n = 5$ independent experiments), respectively. To discriminate between a role for α_{1H} T-type calcium channels in PAP synthesis and PAP release, we assayed PAP in both supernatants and cell lysates of LNCaP cells. A 72-h pretreatment with si- α_{1H2} reduced the basal release of PAP in the incubation buffer by 25% (1 h incubation in HBSS containing 5 mM CaCl_2) and the concentration of PAP contained in the cell lysates by 41% (Fig. 5B). In contrast, the ionomycin-induced PAP secretion was not altered by the si- α_{1H2} pretreatment. Indeed, a 1 h treatment with ionomycin induced a release of PAP corresponding to about 3.4% of the total PAP contained in si-Ctl cell lysates, this figure being unchanged by si- α_{1H2} .

As shown in Fig. 5C, T-type calcium channel inhibitors (20 μM NiCl_2 , 10 μM flunarizine, 500 nM kurtoxin) had no effect on LNCaP-

CTL cells after incubation periods of 1 or 24 h. After 1 h of incubation, the calcium inhibitors had only a limited effect on LNCaP-NE cells, and a slight inhibition was detectable. On the other hand, when LNCaP-NE cells were incubated in the presence of T-type calcium channels inhibitors for 24 h, the enhancement in PAP secretion because of neuroendocrine differentiation was antagonized (Fig. 5C). In addition, Western blot experiments (Fig. 5D) show that the total amount of PAP in LNCaP-NE cells was decreased by T-type calcium channels inhibitors (NiCl_2 , flunarizine, kurtoxin) and by si- α_{1H1} and si- α_{1H2} , confirming a role for α_{1H} -T type calcium channels in PAP synthesis.

We carried out combined electrophysiological and imaging experiments to measure both calcium currents and FM1-43 fluorescence. Although a single depolarizing pulse to 0 mV inducing a calcium current of about 100 pA was not followed by

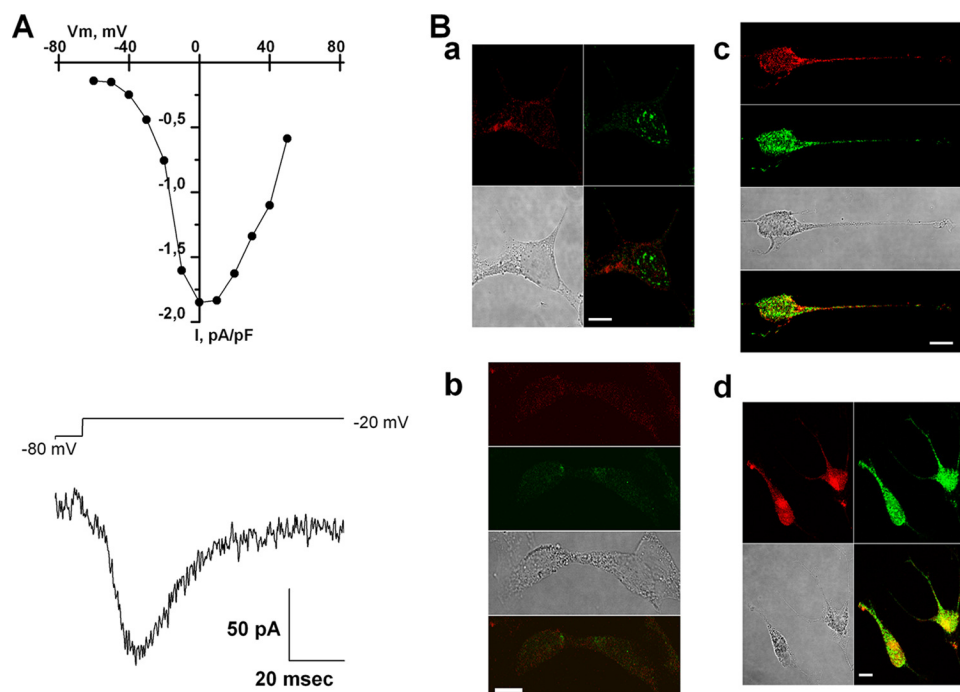


FIGURE 3. T-type calcium channel expression in human prostate neuroendocrine LNCaP cells. *A*, current/voltage (*I/V*) relationship (*top panel*) and example of T-type currents in a typical LNCaP-NE cell (*bottom panel*). Membrane potential was depolarized for 100 ms from -80 mV to -20 mV. *B*, labeling of LNCaP-CTL and LNCaP-NE cells with anti-CaV3.2 (*green* in all panels) and neuroendocrine markers (serotonin or chromogranin A labeled in *red*). Whereas LNCaP-CTL cells did not show any significant fluorescence apart a weak α_{1H} signal into nucleus, LNCaP-NE cells expressed α_{1H} channels and the neuroendocrine markers serotonin and chromogranin A. *a*, LNCaP-CTL cells labeled with anti-chromogranin A (*red*) and anti-CaV3.2 (*green*). *b*, LNCaP-CTL cells labeled with anti-serotonin (*red*) and anti-CaV3.2 (*green*). *c*, LNCaP-NE cells labeled with anti-chromogranin A (*red*) and anti-CaV3.2 (*green*) *d* LNCaP-NE cells labeled with anti-serotonin (*red*) and anti-CaV3.2 (*green*). Bar, 10 μ m.

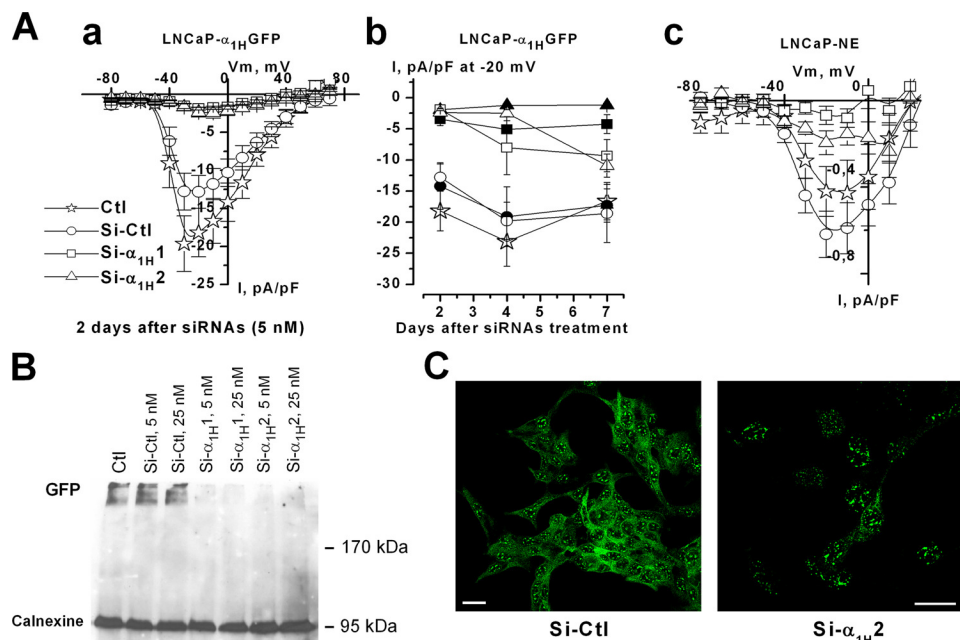


FIGURE 4. Knock-down of α_{1H} calcium channels by siRNAs inhibits voltage-dependent T-type calcium currents in LNCaP cells. siRNAs were used to knock down the expression of α_{1H} T-type calcium channels (si- $\alpha_{1H}1$ and si- $\alpha_{1H}2$) and compared with the action of control siRNA (si-Ctl). *A*, *a*, IV curves carried out on LNCaP- α_{1H} GFP cells representing the peak T-type calcium current density (pA/picofarads (pF)) as a function of membrane potential (mV) and showing the effects of siRNAs against α_{1H} calcium channels 2 days after transfection. *b*, kinetics of siRNAs action on T-type calcium current density at 5 nM (*open symbols*) and 25 nM (*filled symbols*) for a membrane potential of -20 mV (peak of calcium current). *c*, IV curves carried out on LNCaP-NE cells showing the effects of siRNAs against α_{1H} calcium channels 3–4 days after transfection. *B*, action of siRNAs on the expression of α_{1H} GFP protein assessed by Western blotting. *C*, immunofluorescence showing siRNA-mediated silencing (si- $\alpha_{1H}2$, 20 nM) of α_{1H} in LNCaP- α_{1H} cells. Control cells have been treated with control siRNA (20 nM). Bar, 10 μ m.

an increase in FM1-43 fluorescence, a train of voltage pulses to 0 mV at a frequency of 0.5 Hz was seen to produce an increase in FM1-43 fluorescence ($6.5 \pm 3.1\%$ of increase, $n = 5$, Fig. 6A). This increase in FM1-43 fluorescence was inhibited by NiCl_2 (10 μM) and did not occur when the depolarization was set at 80 mV, which is close to the equilibrium potential for calcium (Fig. 6B). Because it has previously been shown that stimulation of protein kinase C by phorbol 12-myristate 13-acetate (PMA) activates T-type calcium channels in human embryonic kidney cells transfected with the α_{1H} subunit (28), we tested whether PMA could activate T-type calcium channels in LNCaP-NE cells and whether it could induce a calcium rise. As shown in Fig. 6C, 100 nM PMA increased the magnitude of the calcium current measured at -20 mV by 100%. IV curve analysis shows that PMA had a stimulatory action mainly at negative potentials between -60 and -10 mV (Fig. 6C) with a 4-fold stimulation at -40 mV (-25 ± 3 pA versus -99 ± 20 pA, $n = 6$). In Fura2 imaging experiments, PMA slowly increased intracellular calcium ($\Delta[\text{Ca}^{2+}]_i = 20.5 \pm 1.3$ nM) in 47% of LNCaP-NE cells ($n = 158$ of 341). This increase in intracellular calcium was antagonized by NiCl_2 (10 μM , Fig. 6D) or by flunarizine (10 μM , not shown) in 90% of the cells tested (110 of 121). We carried out combined imaging experiments with FM1-43 and Fura2 to assess whether this calcium increase could promote secretion. As shown on Fig. 6D, when PMA was applied, the increase in intracellular free calcium concentration was followed by an increase in FM1-43 fluorescence in 60.7% of the LNCaP cells showing an increase in $[\text{Ca}^{2+}]_i$ ($\Delta F_{510\text{nm}} = 31.5 \pm 3\%$, $n = 96$ of 158). Furthermore, in 57.5% of FM1-43-responsive LNCaP cells, NiCl_2 (10 μM) antagonized the calcium increase and impeded further increase in FM1-43 fluorescence.

We then carried out a set of experiments to assess whether

T-type Calcium Channels and Prostate Cancer Secretion

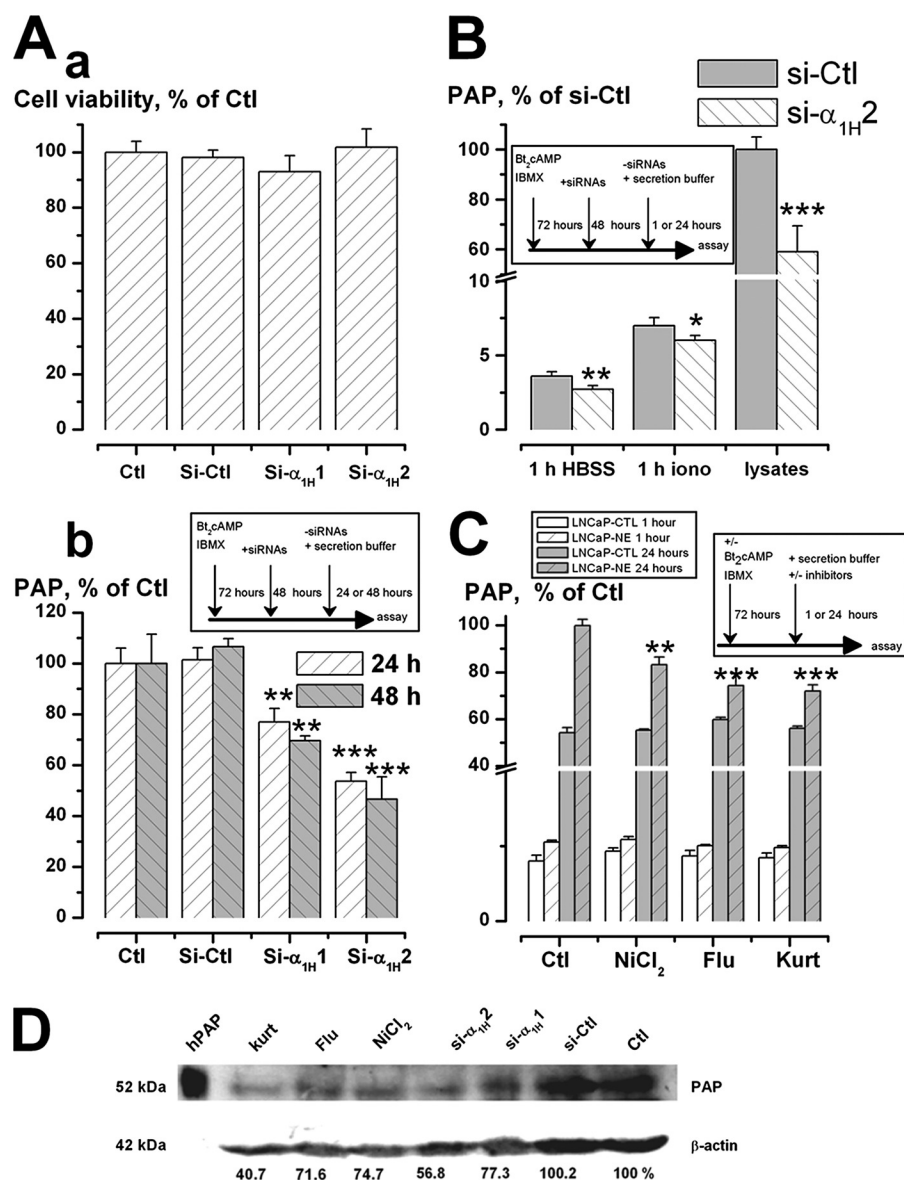


FIGURE 5. T-type calcium channel-dependent secretion of PAP. Knockdown of α_{1H} calcium channels by both siRNAs and calcium channel antagonists inhibit PAP secretion by LNCaP-NE cells. *A*, siRNAs (5 nM) directed against the α_{1H} subunit and control siRNA did not alter cell viability as measured by the incorporation of formazan. *B*, siRNAs (5 nM) against the α_{1H} subunit but not control siRNAs reduced the accumulation of PAP (measured with DIFMUP) secreted by LNCaP-NE cells in the incubation medium (RPMI 1640 and 10% fetal bovine serum) for 24 and 48 h. Data were normalized to the amount of PAP released by control (Ctl) cells. *B*, PAP was assayed using DIFMUP in lysates of cells cultured for 72 h in the presence of si-Ctl or si- α_{1H} 2 (lysates column) and in supernatants (1 h HBSS and 1 h ionomycin (*iono*) columns) of LNCaP-NE cells cultured for 72 h in the presence of si-CTL or si- α_{1H} 2 further treated for 1 h with HBSS alone (containing 5 mM CaCl₂) or with ionomycin (2 μ M). The total amounts of PAP contained in cell lysates and in supernatants were reduced after a 72-h treatment with si- α_{1H} 2. Data were normalized to the total amount of PAP in si-Ctl cell lysates. *Bt₂cAMP*, dibutyryl cAMP; *IBMX*, isobutylmethylxanthine. *C*, concentrations of PAP (%), measured with DIFMUP) released in the RPMI culture medium by LNCaP and LNCaP-NE cells. Cells were incubated for 1 or 24 h with or without calcium channel inhibitors (20 μ M NiCl₂, 10 μ M flunarizine (*Flu*), 500 nM kurtoxin (*Kurt*)). Data were normalized to the amount of PAP released by LNCaP-NE cells after 24 h of incubation in the absence of inhibitor. *D*, Western blot of PAP from LNCaP-NE cell lysates after 48 h treatment with 5 nM si-Ctl, si- α_{1H} 1 or si- α_{1H} 2, 20 μ M NiCl₂, 10 μ M flunarizine, 500 nM kurtoxin. Human PAP (*hPAP*, 0.5 nM) was added in the first lane as a positive control. Average PAP spot intensities were normalized to the average intensities of β -actin used as an internal control. The PAP/ β -actin ratio for each condition (in %) normalized to the control condition (Ctl) is shown below.

human prostatic cells in primary culture express such T-type calcium channels. As shown in Fig. 7, human prostatic cells express functional T-type calcium channels generating voltage-dependent calcium currents. Human prostatic cell calcium currents were blocked by 10 μ M NiCl₂, which is indicative of α_{1H}

T-type calcium channels (29). Reverse transcription-PCR experiments carried out on prostatic tissues obtained after surgery show that tissues from most patients (here, three patients with BHP and 3 patients with prostate carcinoma (PC)) expressed the transcript for CaV3.2 channel (Fig. 7C). In addition, reverse transcription-PCR experiments performed on epithelial cells obtained from human prostate tissue samples and maintained in culture for several days showed the expression of the transcript for CaV3.2 in two batches of epithelial cells from BHP (PrPE1 and PrPE2) and two from PC (PrPC1 and PrPC2). In our experiments 16.2 \pm 2.9% of prostate cancer epithelial cells ($n = 12$ of 74 cells, three different patients) displayed functional T-type calcium currents. None of the cells from BHP tissues expressed a functional T-type current ($n = 0$ of 54 cells, two patients). An immunofluorescence study of CaV3.2 calcium channels and cytokeratin 18 (CK18) was carried out in hyperplastic or cancerous prostate tissues. We show here (Fig. 7D) that there was no CaV3.2 immunostaining detectable above background in hyperplastic acini, whereas there were epithelial cells strongly labeled with the anti-CaV3.2 antibody in cancer acini. Moreover, there was a partial colocalization of CaV3.2 and CK18 immunostaining in the epithelium, meaning that CK18-positive cells were in some cases immunopositive for CaV3.2.

Co-immunostaining with anti-serotonin or anti-chromogranin A antibodies showed that cells expressing CaV3.2 channels are immunopositive for these neuroendocrine markers (Fig. 8). Furthermore, because prostate cancers usually display multiple cancer foci in a same gland, we were able to compare in a same surgical sample glandular areas showing no sign of cancer foci (tissue well differentiated, grade 1) and prostate areas displaying obvious signs of cancer development (dedifferentiation and disorganization of the epithelium, grades 2–4). We then observed that CaV3.2-positive neuroendocrine cells were consistently

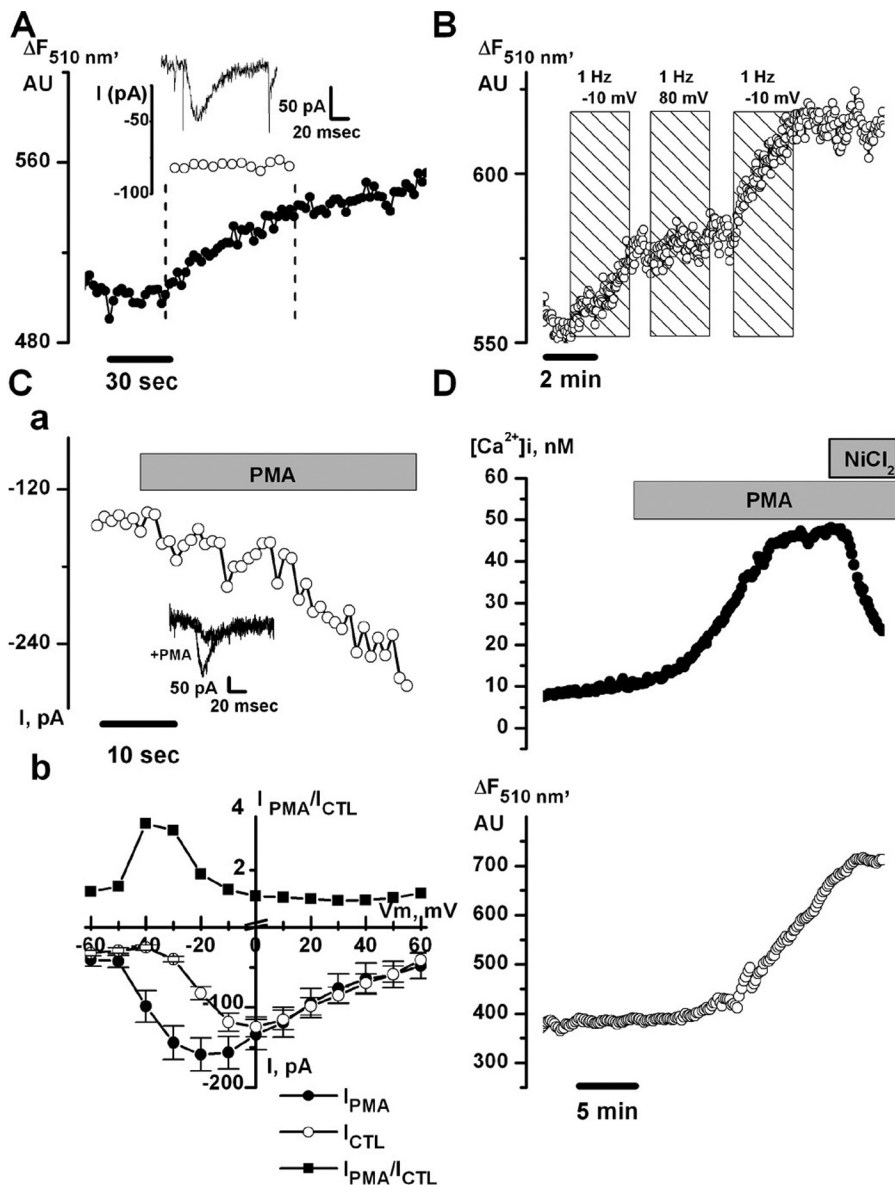


FIGURE 6. **Combined patch clamp or calcium imaging and FM1-43 measurements on LNCaP-NE cells.** *A*, a neuroendocrine LNCaP cell was recorded in whole-cell configuration. FM1-43 was present in the recording medium. At the first dashed vertical bar, the cell was depolarized from -80 to -10 mV at a frequency of 0.5 Hz until the second vertical bar. During that period FM1-43 fluorescence and calcium currents were recorded (typical current and time course shown in the inset between the vertical dashed lines). *B*, a similar experiment performed on a different LNCaP-NE cell. The cell was submitted to three consecutive depolarization trains, the first one at -10 mV (peak value for T-type calcium currents), a second one at 80 mV (close to the reversal potential for calcium), and a third one at -10 mV. *C*, *a*, time-course of T-type calcium currents stimulation by PMA (100 nM) in a typical LNCaP-NE cell. The average current-voltage relationship is shown in *b*. The curve on the top represents the ratio of the current induced by depolarization after PMA stimulation divided by the current recorded in control conditions (before PMA). CTL, control. *D*, combined recording on a single LNCaP-NE cell of cytosolic calcium concentration (top curve) and FM1-43 fluorescence (bottom curve). FM1-43 (5 μ M) was present throughout the experiment in the bathing solution. PMA induced an increase in $[Ca^{2+}]_i$, and FM1-43 fluorescence, which were both antagonized by $NiCl_2$ (10 μ M). AU, absorbance units.

localized in cancerous areas but not in hyperplastic or healthy zones.

DISCUSSION

We have previously shown that a prostate cancer cell line model, namely LNCaP cells, displays functional T-type calcium currents due to the presence of an α_{1H} calcium channel subunit (11, 16). Furthermore, we have shown that their expression is

increased by neuroendocrine differentiation, which is allegedly associated with a poor prognosis (6, 30). Voltage-dependent calcium channels are also expressed in normal rat prostate cells (31), and it has been shown that other T-type calcium channels (α_{1G}) are underexpressed in prostate cancer because of CACNA1G gene hypermethylation (32). In addition, we show here that α_{1H} T-type calcium channels are expressed in human prostate tissues biopsies. Furthermore, we were only able to detect T-type calcium currents in hPCE cells, yet not in BHP cells. In the latter, although the amplicon for CaV3.2 is present, the density of T-type calcium channels may be too low to be detectable. Immunofluorescence experiments show that there is no significant CaV3.2 signal in hyperplastic acini, whereas there are epithelial cells intensely labeled with the anti-CaV3.2 antibody in cancer acini. This shows that the expression of CaV3.2 is certainly higher in prostate cancer than in hyperplasia. In addition, we show that these CaV3.2-positive cells are chromogranin A- and 5HT-positive and present neurite extensions toward the epithelium, which shows their neuroendocrine nature and probably their role in paracrine secretion. The fact that CaV3.2-positive cells are also positive for CK18 reveals that these cells certainly constitute a cell phenotype derived from epithelial cells by transdifferentiation. We cannot exclude that the absence of detectable T-type calcium currents in BHP cells could be due to a difference in the expression of regulatory subunits like γ_4 and $\alpha_2\delta_2$ that we have detected in all prostate cell lines³ between cancer and hyperplastic tissues.

The role of T-type calcium channels in peripheral tissues and specifically in the prostate is still elusive. We have investigated here whether α_{1H} T-type calcium channels could be involved in regulated secretion. We show in this article that LNCaP cells display a calcium-dependent path-

³ F. Gackière, G. Bidaux, P. Delcourt, F. Van Coppenolle, M. Katsogiannou, E. Dewailly, A. Bavencoffe, M. Tran Van Chuoi-Mariot, B. Mauroy, N. Prevarskaya, and P. Mariot, personal observations.

T-type Calcium Channels and Prostate Cancer Secretion

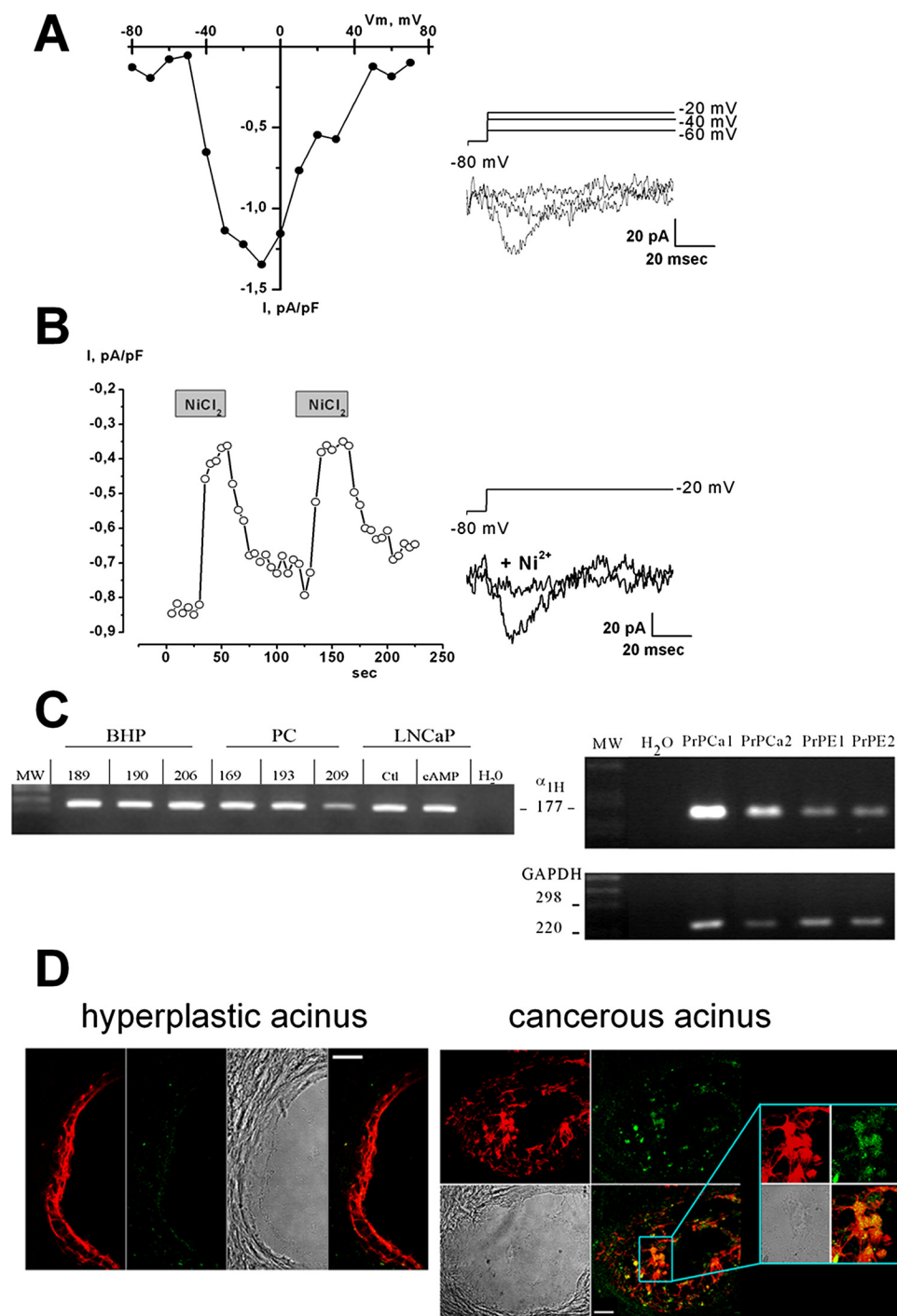


FIGURE 7. T-type calcium channel expression in human prostate cells. *A*, examples of membrane currents in a human prostate carcinoma cell (PrPC, *right panel*). Membrane potential was depolarized for 100 ms from -80 mV to $-20/-40/-60$ mV. The current/voltage (I/V) relationship for this cell is shown on the *left panel*. *pF*, picofarads. *B*, membrane currents before and after the addition of NiCl_2 ($10 \mu\text{M}$) in the recording medium (*right panel*) and time course of the inhibition of T-type calcium currents by NiCl_2 ($10 \mu\text{M}$) in a PrPC cell (*left panel*). *C*, *left panel*, agarose gel showing the expression of the α_{1H} amplicon (expected size, 177 bp) in a prostate cell line (LNCaP) treated or not with dibutyryl cAMP for 3 days, three different prostate benign hyperplasia tissues (BHP), and three different human prostatic carcinoma tissues (PC). MW, molecular weight. *Right panel*, expression of the α_{1H} amplicon in human prostate epithelial cells (PrPE) and human prostate cancer cells (PrPCa) obtained from surgery samples in primary culture. A no-template control (H_2O) was also run with the PCR samples, where the cDNA was replaced with water. A 1-kilobase DNA ladder (MW (bp)) was used as a DNA size marker. GAPDH, glyceraldehyde-3-phosphate dehydrogenase. *D*, *left panel*, immunofluorescence of prostate benign hyperplasia showing the presence of the apical epithelial marker cytokeratine 18 (red) but no significant α_{1H} fluorescence (green) in an acinus. *Right panel*, confocal slide of a representative cancerous acinus (objective $\times 40$). Cancerous apical epithelial cells invading the lumen are detected with cytokeratine 18 (red). An islet of α_{1H} -positive apical epithelial cells (green) is detected in the epithelium near the center of the lumen (*left panel*). Interestingly, these apical epithelial neuroendocrine-like cells emit neurite lengthenings toward cancerous apical epithelial cells (*right panel*, magnification). Bar, $10 \mu\text{m}$.

way of regulated secretion and that neuroendocrine differentiation is associated with an increase in T-type calcium channel-dependent PAP secretion.

To assay secretion in prostate cancer cells, we chose to monitor PAP released in the culture medium. We initially attempted to measure the secretion of neuropeptides (neurotensin and parathyroid hormone-related peptide) by LNCaP-NE cells as performed by others (27). Although we used essentially the same enzyme-linked immunosorbent assay kits (Peninsula) and the same culture conditions, we were unable to detect any secretion of either neurotensin or parathyroid hormone-related peptide in even stimulated (ionomycin) conditions. PAP is one of the main secretory products released by prostate cells with prostate-specific antigen (PSA) and was shown to exist in two forms, an intracellular (cPAP) and a secreted one (sPAP), the latter being localized in secretory granules of prostate cells (for review, see Ref. 33) and released upon stimuli like protein kinase C activation in LNCaP cells (25). Until now, it was yet to be shown that its secretion is finely regulated by calcium. Here, we show that various pharmacological agents (thapsigargin, ionomycin) raising cytosolic free calcium concentration to several micromolar are able to promote PAP release within periods short enough (30 min) to stimulate intracellular trafficking and exocytosis. In addition, short-term enhancement of PAP secretion by ionomycin was not abolished by protein synthesis inhibitors, showing that early PAP secretion was mostly dependent on exocytosis stimulation. We also show here that long-lasting calcium stimulations (24 h) promote PAP synthesis and its release into the extracellular milieu. Calcium-dependent secretion was confirmed in LNCaP cells using FM1-43 and TMA-DPH imaging assays. These lipophilic dyes have been widely used to measure exocytotic release in neurons, endocrine, or exocrine

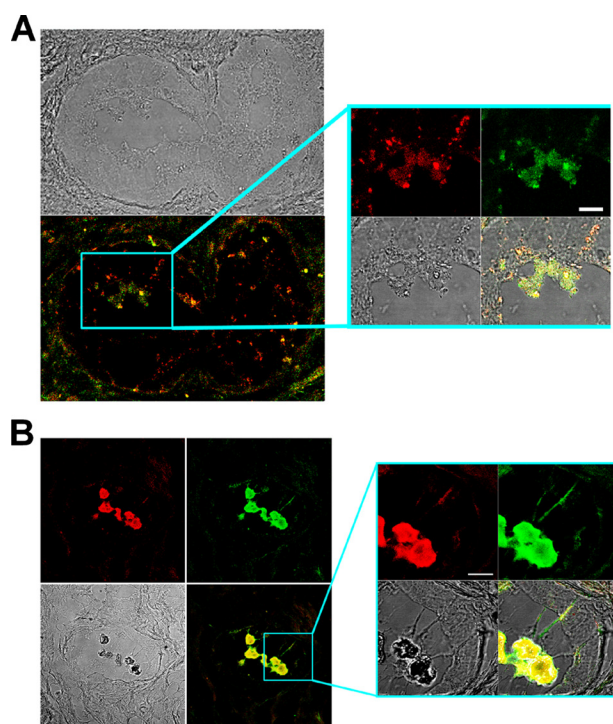


FIGURE 8. Coimmunostaining with anti-CaV3.2 antibody and antibodies against neuroendocrine markers in prostate cancer samples. Transdifferentiated cancerous apical epithelial cells expressed both neuroendocrine marker chromogranin A and serotonin and α_{1H} channel. *A*, immunohistofluorescence of a prostate cancerous acinus (grade 2) showing the expression of neuroendocrine marker chromogranin A (red) and α_{1H} fluorescence (green) in an islet of apical epithelial cells. *B*, detection of serotonin (red) and α_{1H} (green) proteins in apical epithelial cells of a prostate cancerous acinus (grade 3–4). Bar, 10 μ m.

cells (21, 22, 34). As noticed from our experiments, FM1-43 fluorescence increased after ionomycin or thapsigargin stimulation in the absence or presence of extracellular calcium, although more efficiently in the latter condition. This reflects that both ionomycin and thapsigargin are able to promote calcium release from internal stores, which in turn was sufficient enough to trigger exocytosis. This could be followed in the presence of external calcium by a calcium entry through plasma membrane calcium channels which was more potent to stimulate exocytosis.

We then investigated whether calcium-dependent secretion could be stimulated by calcium entry through T-type calcium channels in LNCaP-NE cells. We first showed that LNCaP-NE cells secrete more PAP than non-differentiated cells. Basal PAP secretion by LNCaP-NE cells depends on calcium entry through α_{1H} T-type calcium since PAP secretion was inhibited by nickel chloride at micromolar concentrations and by flunarizine. In addition, PAP secretion decreased in LNCaP-NE cells that had been transfected with siRNA raised against α_{1H} subunits. We also show that both basal release and PAP synthesis were diminished by siRNA treatments. On the other hand, the secretion capacity in response to another stimulus (*i.e.* ionomycin) was not altered by siRNA incubations, which shows that knocking down the expression of α_{1H} calcium channels does not probably induce any down-regulation of other proteins involved in exocytosis. It, therefore, seems that part of the PAP secreted by LNCaP-NE cells may be due to calcium entry

through α_{1H} T-type calcium channels. As can be observed from our experiments, inhibition of CaV3.2 channels by either siRNAs or inhibitors does not totally abolish PAP secretion. This may reflect the participation of other calcium channels in secretion such as TRPV6 channels, which have been shown to be expressed in prostate LNCaP cells and to participate to basal calcium entry (35). In addition, we confirm that T-type calcium channels can be activated by phorbol esters (PMA) as previously shown by others (28). More importantly, we show that this activation could promote exocytosis as measured by FM1-43 fluorescence increase. This response was antagonized by nickel chloride and flunarizine in a significant portion of cells, showing the involvement of T-type calcium channels in PMA-induced exocytosis. We also show, using combined electrophysiological and imaging experiments, that depolarization trains leading to the activation of T-type voltage-dependent calcium channels were able to increase FM1-43 fluorescence. Because the α_{1H} (CaV3.2) subunit is the only voltage-dependent calcium channel expressed in prostate cancer LNCaP cells (11), we assume that this calcium channel subunit is responsible for exocytosis. Such a role for T-type calcium channels is beginning to emerge since their activation stimulates exocytosis as measured with capacitance measurements in various excitable cellular systems (36) such as retinal bipolar neurons (15). In neuroendocrine cells, it seems that T-type calcium channels are also functionally coupled to dense core granules containing neurohormones with similar efficiency to HVA calcium channels (37). In addition, because we have observed that chromogranin A, a marker of regulated secretion and serotonin, is expressed by LNCaP-NE and neuroendocrine cells in prostate cancerous acini, we may speculate that there is a regulated secretion of serotonin by these neuroendocrine prostate cancer cells and that CaV3.2 T-type calcium channels could participate in its secretion.

T-type calcium channels may play their part in secretion when activated by transient membrane depolarizations or when they are open at resting membrane potentials, thereby promoting a steady-state calcium entry. As previously shown, LNCaP-NE cells have an average calcium concentration increased by about 20 nM as compared with LNCaP-CTL (11). This difference in calcium concentration is probably locally underestimated since calcium entry through T-type calcium channels almost definitely increases calcium concentration in restricted areas nearby the plasma membrane. This sustained calcium entry through T-type calcium channels may certainly be responsible for the increased PAP secretion observed in LNCaP-NE cells. It is likely that basal calcium entry at resting membrane potential is the main function of T-type calcium channels in prostate cancer cells since we have never observed any action potentials or calcium spikes in LNCaP-NE cells. However, we cannot exclude that action potential firing may not be of physiological relevance in normal epithelial prostate cells since others have published that rat neuroendocrine epithelial prostate cells display membrane excitability (31) and that there is a spontaneous electrical activity in the prostate gland probably due to pacemaker interstitial cells similar to that of intestinal interstitial cells of Cajal (38). Spontaneous electrical activity initiated in the interstitial cells could, therefore,

T-type Calcium Channels and Prostate Cancer Secretion

spread to epithelial cells. If this was true, T-type calcium channels could serve in this context for triggering secretion during action potentials.

In LNCaP neuroendocrine prostate cancer cells, the α_{1H} calcium channel subunit is, therefore, able to promote PAP synthesis and release. It has been shown that neuroendocrine cells in human prostate cancer tissues, positive for neuroendocrine markers like chromogranin A, expressed and could secrete PAP but were negative for PSA (39) and Ki-67, a marker of proliferation (40). As also illustrated by our data, neuroendocrine cells in human prostate cancer, therefore, share some properties with epithelial cells (expression of CK18 for instance) and could secrete both PAP and neuropeptides. In our experiments, neuroendocrine cells could secrete PAP and probably serotonin, which has been characterized to be a mitogenic factor and the expression of which is correlated with a poor prognosis (41). The situation seems to be somehow quite different in normal human prostate tissues where neuroendocrine cells do not express any of the PAP and PSA epithelial markers (42). The role of PAP during the pathological development of the prostate cancer is not clear due to the presence of two different forms of PAP, with different physicochemical properties (cPAP and sPAP). Indeed, during the development of prostate cancer, the concentration of sPAP, whose role remains elusive, rises in the serum. This led to the utilization of cPAP as a molecular marker of prostate cancer for many years before the discovery of PSA as a more reliable, if not perfect, marker. However, it has been recently suggested that the contribution of PAP screening should be reevaluated in the light of recent results showing that secretion of PAP in the serum may constitute a prognostic factor for patients with high risk cancer (43). On the contrary, the expression of cPAP seems to be inversely correlated with prostate carcinogenesis (for review, see Ref. 33). In addition, it has been shown that cPAP reduces cell proliferation by decreasing tyrosine phosphorylation of HER2, a member of the Erb receptor protein-tyrosine kinase family (44). Furthermore, it has been suggested that PAP secreted in the serum could participate through a stimulation of collagen and alkaline phosphatase in the bone to the sclerosis of bone tissue in the vicinity of cancerous prostatic metastases (45).

Alterations in secretory pathways have been suggested, and proteins involved in the exocytotic machinery responsible for PAP and PSA secretion are beginning to be described. For instance, JFC1, a synaptotagmin-like protein highly expressed in prostate tissue, is involved in PAP and PSA secretion and is activated by NF- κ B and phosphatidylinositol 3-kinase, which are both frequently up-regulated in prostate cancer (46). This strengthens the role of CaV3.2 T-type calcium channels in secretion by prostate neuroendocrine cells since synaptotagmin-like proteins are known to be calcium sensors involved in regulated secretion through a functional coupling with voltage-gated calcium channels.

In our experiments, because α_{1H} T-type calcium channels promote both PAP synthesis and secretion, we speculate that these channels may participate in the perturbation of PAP secretion during prostate cancer development. In a more general sense, α_{1H} T-type calcium channels may enhance auto-crine/paracrine secretion in neuroendocrine prostate cancer

cells in which they are overexpressed (47). We suggest that these channels, by promoting the secretion of potentially mitogenic factors such as neuropeptides or serotonin by neuroendocrine cells, could be responsible for the progression of prostate cancer toward an androgen-independent stage. In this context, it is noteworthy that these channels are suspected of promoting proliferation of glioma (48) or esophageal carcinoma cells (49) and that they have been shown to be potential markers of breast cancer (50).

REFERENCES

1. Feldman, B. J., and Feldman, D. (2001) *Nat. Rev. Cancer* **1**, 34–45
2. Weinstein, M. H., Partin, A. W., Veltri, R. W., and Epstein, J. I. (1996) *Hum. Pathol.* **27**, 683–687
3. Bonkhoff, H., Wernert, N., Dhom, G., and Remberger, K. (1991) *Prostate* **19**, 91–98
4. Bonkhoff, H. (1998) *Prostate* (suppl. 8) 18–22
5. Theodoropoulos, V. E., Tsigka, A., Mihalopoulou, A., Tsoukala, V., Lazaris, A. C., Patsouris, E., and Ghikonti, I. (2005) *Urology* **66**, 897–902
6. Cohen, R. J., Glezeron, G., Haffjee, Z., and Afrika, D. (1990) *Br. J. Urol.* **66**, 405–410
7. Yuan, T. C., Veeramani, S., Lin, F. F., Kondrikou, D., Zelivianski, S., Igawa, T., Karan, D., Batra, S. K., and Lin, M. F. (2006) *Endocr. Relat. Cancer* **13**, 151–167
8. Bang, Y. J., Pirmia, F., Fang, W. G., Kang, W. K., Sartor, O., Whitesell, L., Ha, M. J., Tsokos, M., Sheahan, M. D., Nguyen, P., Niklinski, W. T., Myers, C. E., and Trepel, J. B. (1994) *Proc. Natl. Acad. Sci. U. S. A.* **91**, 5330–5334
9. Cox, M. E., Deeble, P. D., Bissonette, E. A., and Parsons, S. J. (2000) *J. Biol. Chem.* **275**, 13812–13818
10. Zelivianski, S., Verni, M., Moore, C., Kondrikov, D., Taylor, R., and Lin, M. F. (2001) *Biochim. Biophys. Acta* **1539**, 28–43
11. Mariot, P., Vanoverberghe, K., Lalevee, N., Rossier, M. F., and Prevarskaya, N. (2002) *J. Biol. Chem.* **277**, 10824–10833
12. Darszon, A., Lopez-Martinez, P., Acevedo, J. J., Hernandez-Cruz, A., and Trevino, C. L. (2006) *Cell Calcium* **40**, 241–252
13. Carbone, E., Giaccipoli, A., Marcantoni, A., Guido, D., and Carabelli, V. (2006) *Cell Calcium* **40**, 147–154
14. Giaccipoli, A., Novara, M., de Luca, A., Baldelli, P., Marcantoni, A., Carbone, E., and Carabelli, V. (2006) *Biophys. J.* **90**, 1830–1841
15. Pan, Z. H., Hu, H. J., Perring, P., and Andrade, R. (2001) *Neuron* **32**, 89–98
16. Gackiere, F., Bidaux, G., Lory, P., Prevarskaya, N., and Mariot, P. (2006) *Cell Calcium* **39**, 357–366
17. Thebault, S., Roudbaraki, M., Sydorenko, V., Shuba, Y., Lemonnier, L., Slomianny, C., Dewailly, E., Bonnal, J. L., Mauroy, B., Skryma, R., and Prevarskaya, N. (2003) *J. Clin. Invest.* **111**, 1691–1701
18. Bidaux, G., Roudbaraki, M., Merle, C., Crepin, A., Delcourt, P., Slomianny, C., Thebault, S., Bonnal, J. L., Benahmed, M., Cabon, F., Mauroy, B., and Prevarskaya, N. (2005) *Endocr. Relat. Cancer* **12**, 367–382
19. Gryniewicz, G., Poenie, M., and Tsien, R. Y. (1985) *J. Biol. Chem.* **260**, 3440–3450
20. Brumback, A. C., Lieber, J. L., Angleson, J. K., and Betz, W. J. (2004) *Methods* **33**, 287–294
21. Cochilla, A. J., Angleson, J. K., and Betz, W. J. (1999) *Annu. Rev. Neurosci.* **22**, 1–10
22. Masumoto, N., Tasaka, K., Mizuki, J., Fukami, K., Ikebuchi, Y., and Miyake, A. (1995) *Cell Calcium* **18**, 223–231
23. Nunez, L., Villalobos, C., Boockfor, F. R., and Frawley, L. S. (2000) *Endocrinology* **141**, 2012–2017
24. Hamill, O. P., Marty, A., Neher, E., Sakmann, B., and Sigworth, F. J. (1981) *Pfluegers Arch. Eur. J. Physiol.* **391**, 85–100
25. Lin, M. F., Zhang, X. Q., Dean, J., and Lin, F. F. (2001) *Cell Biol. Int.* **25**, 1139–1148
26. Gee, K. R., Sun, W. C., Bhalgat, M. K., Upson, R. H., Klaubert, D. H., Latham, K. A., and Haugland, R. P. (1999) *Anal. Biochem.* **273**, 41–48
27. Cox, M. E., Deeble, P. D., Lakhani, S., and Parsons, S. J. (1999) *Cancer Res.* **59**, 3821–3830

T-type Calcium Channels and Prostate Cancer Secretion

28. Park, J. Y., Jeong, S. W., Perez-Reyes, E., and Lee, J. H. (2003) *FEBS Lett.* **547**, 37–42
29. Lee, J. H., Gomora, J. C., Cribbs, L. L., and Perez-Reyes, E. (1999) *Biophys. J.* **77**, 3034–3042
30. Cohen, R. J., Glezeron, G., and Haffeejee, Z. (1991) *Br. J. Urol.* **68**, 258–262
31. Kim, J. H., Shin, S. Y., Yun, S. S., Kim, T. J., Oh, S. J., Kim, K. M., Chung, Y. S., Hong, E. K., Uhm, D. Y., and Kim, S. J. (2003) *Pfluegers Arch. Eur. J. Physiol.* **446**, 88–99
32. Toyota, M., Ho, C., Ohe-Toyota, M., Baylin, S. B., and Issa, J. P. (1999) *Cancer Res.* **59**, 4535–4541
33. Veeramani, S., Yuan, T. C., Chen, S. J., Lin, F. F., Petersen, J. E., Shaheduz-zaman, S., Srivastava, S., MacDonald, R. G., and Lin, M. F. (2005) *Endocr. Relat. Cancer* **12**, 805–822
34. Shorte, S. L., Stafford, S. J., Bamford, M., Collett, V. J., and Schofield, J. G. (1993) *J. Physiol. (Lond.)* **470**, 191–210
35. Lehen'kyi, V., Flourakis, M., Skryma, R., and Prevarskaya, N. (2007) *Oncogene* **26**, 7380–7385
36. Carbone, E., Marcantoni, A., Giaccipoli, A., Guido, D., and Carabelli, V. (2006) *Pfluegers Arch. Eur. J. Physiol.* **453**, 373–383
37. Mansvelder, H. D., and Kits, K. S. (2000) *J. Physiol. (Lond.)* **526**, 327–339
38. Exintaris, B., Nguyen, D. T., Dey, A., and Lang, R. J. (2006) *Auton. Neurosci.* **126–127**, 371–379
39. Cohen, R. J., Glezeron, G., and Haffeejee, Z. (1992) *Arch. Pathol. Lab. Med.* **116**, 65–66
40. Huang, J., Yao, J. L., di Sant'Agnese, P. A., Yang, Q., Bourne, P. A., and Na, Y. (2006) *Prostate* **66**, 1399–1406
41. Dizayi, N., Bjartell, A., Nilsson, E., Hansson, J., Gadaleanu, V., Cross, N., and Abrahamsson, P. A. (2004) *Prostate* **59**, 328–336
42. Aumuller, G., Leonhardt, M., Janssen, M., Konrad, L., Bjartell, A., and Abrahamsson, P. A. (1999) *Urology* **53**, 1041–1048
43. Taira, A., Merrick, G., Wallner, K., and Dattoli, M. (2007) *Oncology (Wil-liston Park)* **21**, 1003–1010
44. Meng, T. C., and Lin, M. F. (1998) *J. Biol. Chem.* **273**, 22096–22104
45. Ishibe, M., Rosier, R. N., and Puzas, J. E. (1991) *J. Clin. Endocrinol. Metab.* **73**, 785–792
46. Johnson, J. L., Ellis, B. A., Noack, D., Seabra, M. C., and Catz, S. D. (2005) *Biochem. J.* **391**, 699–710
47. Chemin, J., Nargeot, J., and Lory, P. (2004) *Neuroreport* **15**, 671–675
48. Panner, A., Cribbs, L. L., Zainelli, G. M., Oritano, T. C., Singh, S., and Wurster, R. D. (2005) *Cell Calcium* **37**, 105–119
49. Lu, F., Chen, H., Zhou, C., Liu, S., Guo, M., Chen, P., Zhuang, H., Xie, D., and Wu, S. (2007) *Cell Calcium* **43**, 49–58
50. Asaga, S., Ueda, M., Jinno, H., Kikuchi, K., Itano, O., Ikeda, T., and Kitajima, M. (2006) *Anticancer Res.* **26**, 35–42